

MS No. S-2013-022.R2

Design Implications of Large-Scale Shake-Table Test on Four-Story Reinforced Concrete Building

by T. Nagae, W. M. Ghannoum, J. Kwon, K. Tahara, K. Fukuyama, T. Matsumori, H. Shiohara, T. Kabeyasawa, S. Kono, M. Nishiyama, R. Sause, J. W. Wallace, and J. P. Moehle

A full-scale, four-story, reinforced concrete building designed in accordance with the current Japanese seismic design code was tested under multi-directional shaking on the E-Defense shake table. A two-bay moment frame system was adopted in the longer plan direction and a pair of multi-story walls was incorporated in the exterior frames in the shorter plan direction. Minor adjustments to the designs were made to bring the final structure closer to U.S. practice and thereby benefit a broader audience. The resulting details of the test building reflected most current U.S. seismic design provisions. The structure remained stable throughout the series of severe shaking tests, even though lateral story drift ratios exceeded 0.04. The structure did, however, sustain severe damage in the walls and beam-column joints. Beams and columns showed limited damage and maintained core integrity throughout the series of tests. Implications of test results for the seismic design provisions of ACI 318-11 are discussed.

Keywords: collapse; damage; design; full-scale; moment frame; multi-story; shake table; shear wall.

INTRODUCTION

Code requirements for reinforced concrete have evolved significantly around the world in the past decades. In the United States, the 1971 San Fernando, CA, earthquake was a watershed event leading to the introduction of requirements for ductile reinforced concrete buildings, which have evolved incrementally since that time based on field and laboratory experiences. In Japan, following a history of several damaging earthquakes and many laboratory tests, the Japanese seismic design code was substantially revised in 1981. In the 1995 Hyogoken-Nanbu earthquake, many reinforced concrete buildings designed before 1981 experienced major failures, especially in the first-story columns and walls. Although newer reinforced concrete buildings designed in accordance with the revised 1981 code showed improved resistance against collapse, several sustained severe damage due to their large deformations. Such damage made it difficult to continue using them after the earthquake and resulted in high repair costs. This experience demonstrates that further improvements in seismic design of concrete buildings might be desirable for the future.

It was in light of the aforementioned experiences that a large-scale shake-table testing program was conducted in 2010. Within the program, a full-scale, four-story, reinforced concrete building designed in accordance with the present Japanese seismic design code was tested by using the E-Defense shake table. The main objectives of the study related to the concrete building were: 1) to verify methods for assessing performance such as strength, deformation

capacity, and failure mode; 2) to identify suitable computational methods to reproduce the seismic responses of the building; and 3) to develop a practical method for assessing damage states regarding reparability.

Design and instrumentation of the test structure were performed with input from U.S. co-authors. Wherever possible, minor adjustments to the designs were made to bring the final structure closer to U.S. practice and thereby benefit a broader audience. The resulting details of the test building reflected the most current U.S. seismic design provisions (Nagae et al. 2011b).

Summaries of the global behavior of the test building and key local damage and deformation observations are presented. A comparison between the details of the test structure and U.S. seismic design practices is also provided. Implications of test results for the seismic design provisions of ASCE 7-10 (ASCE/SEI Committee 7 2010) and ACI 318-11 (ACI Committee 318 2011) are discussed. In a related publication (Nagae et al. 2011a), the seismic design provisions of the Architectural Institute of Japan (AIJ 1999) were evaluated in light of test results.

RESEARCH SIGNIFICANCE

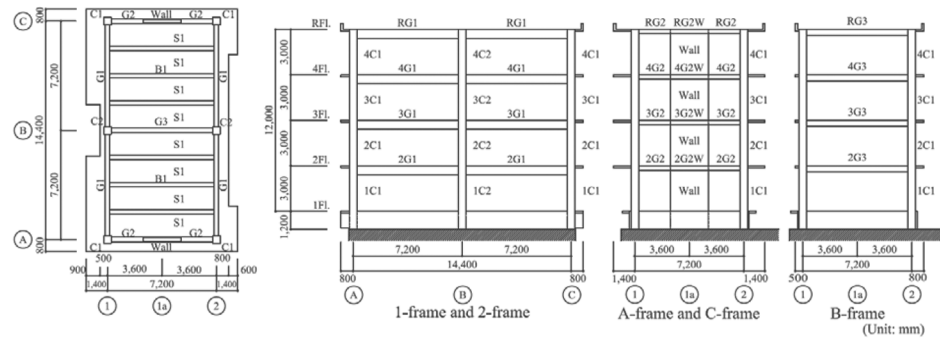
Current Japanese and U.S. seismic design provisions are based on pseudo-dynamic component tests, sub-assembly tests, and limited dynamic tests of partial structural systems. The test presented is a first-of-its-kind, multi-directional, dynamic test of a complete, full-scale reinforced concrete building system to near collapse damage states. The test provides unique data on component and system performance that are used to evaluate current seismic design provisions and highlight potential code changes.

SPECIMEN DETAILS

Figure 1 shows the plans and framing elevations of the reinforced concrete test building. Figure 2 shows a photograph of the test building on the E-Defense shake table. The height of each story is 3 m (118.1 in.). The building footprint measures 14.4 m (47 ft 3 in.) in the longer (X) direction, and 7.2 m (23 ft 7.5 in.) in the shorter (Y) direction. A two-bay moment frame system was adopted in the longer (X) plan direction and a pair of multi-story walls were incorporated

ACI Structural Journal, V. 112, No. 1-6, January-December 2015.

MS No. S-2013-022.R2, doi: 10.14359/51687421, received May 21, 2014, and reviewed under Institute publication policies. Copyright © 2015, American Concrete Institute. All rights reserved, including the making of copies unless permission is obtained from the copyright proprietors. Pertinent discussion including author's closure, if any, will be published ten months from this journal's date if the discussion is received within four months of the paper's print publication.



(a) Columns

(b) Walls

	C1	C2
Top Section		
B x H	500 x 500	
Rebar	8-D22	
Hoop	2,3-D10@100	
Joint	2,2-D10@140	
Bottom Section		
B x H	500 x 500	500 x 500
Rebar	10-D22	10-D22
Hoop	3,4-D10@100	3,4-D10@100
Joint	2,2-D10@140	2,2-D10@140

Section	II	
1Fl.		
B x H	250 X 2,500	
Rebar	2 x 6-D19	Vertical D13@300 (W)
Hoop	2,3-D10@80	Horizontal A D10@125 (W)
Joint	C 2,3-D10@100	C D10@200 (W)
Joint	2,2-D10@150	

(c) Beams

	G1		
Location	End	Center	End
Section			
2Fl.	B x H 300 x 600		
Top	6-D22	3-D22	6-D22
Bottom	3-D22	3-D22	3-D22
Web	4-D10		
Stirrup	2-D10@200		

	G2	
Location	End	Center
Section		
4Fl.	B x H 300 x 300	
3Fl.	3-D19	4-D19
2Fl.	3-D19	3-D19
Stirrup	2-D10@100(KSS785)	

	G3	
Location	End	Center
Section		
2Fl.	B x H 300 x 400	
Top	4-D19	3-D19
Bottom	3-D19	4-D19
Web	2-D10	
Stirrup	2-D10@200	

Example nomenclature for hoop and joint transverse reinforcement: 2,3-D10@100 signifies 2 legs in the H direction and 3 legs in the B direction of D10 bars spaced at 100 mm

Fig. 1—Framing and reinforcing details. (Note: Dimensions are in mm; 1 mm = 0.039 in.)



Fig. 2—Reinforced concrete (left) and prestressed concrete (right) specimens on the E-Defense shake table.

in the exterior frames in the shorter (Y) plan direction. The thickness of the top slab was 130 mm (5.1 in.). Rigid steel frames were set within the open stories of the test specimen for collapse prevention and measurement of story deformations. Representative building mechanical equipment

was incorporated to assess potential damage during strong seismic motions. Table 1 lists the various weights of the test specimen. The weight was estimated based on the reinforced concrete members, the fixed steel frames, and the equipment. Figure 1 shows dimensions and reinforcing details of typical members. The test building was designed in accordance with current Japanese seismic design practice.

When constructing the test building, columns, walls, beams, and the floor slab were cast monolithically. The longitudinal reinforcement of columns, beams, and the wall boundaries were connected by gas pressure welding. Lap splices were used for the reinforcement of other parts of the walls and the floor slabs. The frames in the test building were nominally identical in design and detailing. The shear walls at axes A and C contained the same amount of longitudinal reinforcement but differed in the spacing of transverse reinforcement (Fig. 1). A complete set of drawings and specimen details can be found in Nagae et al. (2011b). Additional test data can be found on the NEEShub website (NEEShub 2011) and in Tuna (2012).

SPECIMEN DESIGN

The extent to which the test structure satisfies the seismic design provisions of ASCE 7-10 and ACI 318-11 is explored

Table 1—Weight and design forces

(A) Structural elements, kN		Roof	Fourth floor	Third floor	Second floor
RC	Column	53	106	106	106
	Beam	240	240	240	240
	Wall	40	79	79	79
	Slab	484	428	424	420
Sum		816	853	849	845
(B) Non-structural elements, kN		Roof	Fourth floor	Third floor	Second floor
Steel	Stair and handrail	6	6	6	6
	Measurement frame	0	3	17	17
Equipment		112	5	0	0
Sum		118	14	23	23
Total of (A) and (B), kN		934	867	872	867
		Fourth story	Third story	Second story	First story
ΣW_i , kN		934	1801	2673	3541
$C_i = 0.2 \times A_i$		0.29	0.25	0.22	0.20
Q_i , kN		273	450	593	708

Notes: 1 kN = 0.225 kip; W_i is weight of floor i ; A_i is shape factor for vertical distribution of lateral forces for floor i ; C_i is lateral force at floor i as a fraction of ΣW_i ; and Q_i is shear at story i .

in this section. The building specimen was designed to withstand the seismic lateral forces presented in Table 1 (MLIT 2007) without members exceeding their elastic limits. These forces, which sum to 20% of the weight of the structure, are higher than those that would be specified by ASCE 7-10 (Section 12.8.1.3), which caps seismic lateral forces for a low-rise building to $1/R$ times the structure weight for a design basis earthquake, where R is the response modification coefficient (8 for special reinforced concrete moment frames and 6 for special reinforced concrete shear walls). The vertical distribution of the design forces, given by the parameter A_i in Table 1, is similar to the ASCE 7-10 specification (approximate inverted triangular distribution).

Results of material tests are given in Tables 2 and 3. In subsequent evaluations, the moment and shear strengths of each member were calculated adopting the compressive strength of concrete and the yield strength of steel reinforcement obtained by averaging material test results.

To aid in the design of the test specimen, pushover (nonlinear static) analyses were conducted on line-element models of the structure. Figure 3 presents pushover results for the final test specimen details. The analytical model used for pushover analyses was built following work by Kabeyasawa et al. (1984). The effective flange width of a top slab was adopted in accordance with the recommendations of the 2007 MLIT Standard. A vertical distribution defined by the parameter A_i (Table 1) was adopted for the lateral force distribution. In the analytical model, inelastic deformations of beam elements were represented by rotational springs at the ends of elements. The first and second break points corresponding to member cracking strength and flexural strength were assigned in the tri-linear moment-rotation

Table 2—Material properties of concrete

	F_c , N/mm ²	σ_B , N/mm ²	E_c , N/mm ²
Cast of fourth story and roof floor slab	27	41.0	30.5
Cast of third story and fourth floor slab	27	30.2	30.3
Cast of second story and third floor slab	27	39.2	32.8
Cast of first story and second floor slab	27	39.6	32.9

Notes: 1 N/mm² = 0.145 ksi; F_c is specified concrete compressive strength; σ_B is measured concrete compressive strength; and E_c is measured secant modulus of concrete.

Table 3—Material properties of steel

	Grade	$A_{nominal}$, mm ²	σ_y , N/mm ²	σ_t , N/mm ²	E_s , kN/mm ²
D22	SD345	387	370	555	209
D19	SD345	287	380	563	195
D13	SD295	127	372	522	199
D10	SD295	71	388	513	191
D10	SD295	71	448	545	188
D10	KSS785	71	952	1055	203

Notes: 1 mm² = 0.0016 in.²; 1 N/mm² = 0.145 ksi; $A_{nominal}$ is nominal area of reinforcing bars; σ_y is measured yield strength of steel reinforcement; σ_t is measured ultimate strength of steel reinforcement; and E_s is measured elastic modulus of steel reinforcement.

relationship. The secant stiffness corresponding to the flexural strength was calculated in accordance with provisions of the MLIT standard (2007). Beyond flexural yielding, the stiffness was reduced to 0.01 times the initial effective stiffness. The pushover analysis indicates that the ultimate base-shear strength of the building specimen is approximately $0.42W$ (1500 kN [337 kip]) in the frame direction and $0.51W$ (1800 kN [405 kip]) in the wall direction.

Figure 4 shows the column-beam moment strength ratios. Reinforcement of the top slab was reflected in the moment strength of beams in negative bending (top in tension). Effective flange widths of beams were adopted in accordance with the recommendations of the 2007 MLIT Standard or ACI 318-11, which produced roughly similar flange widths. Variations of column axial forces due to lateral forces were estimated from pushover analysis in the Japanese calculations. In the U.S. calculations, a plastic mechanism was assumed in which hinging of the columns occurs at the foundation and just below the roof, and beam hinging occurs at column faces at intermediate floors in the frame direction. In the wall direction, the assumed plastic mechanism considered hinging of the columns and walls at the foundation, and beam hinging at column and wall faces. Discrepancies in column-beam moment strength ratios evaluated using ACI and MLIT procedures (Fig. 4) can mostly be attributed to differences in the estimates of axial forces on columns. From the second to fourth floors, the column-beam moment strength ratios were slightly below 1.0 for interior columns, while those of exterior columns ranged from approximately 1.0 to 1.87.

Assessment of specimen design in accordance with U.S. seismic design practice

The structure was assessed in both the X and Y directions using ACI 318-11 and ASCE 7-10 provisions. The

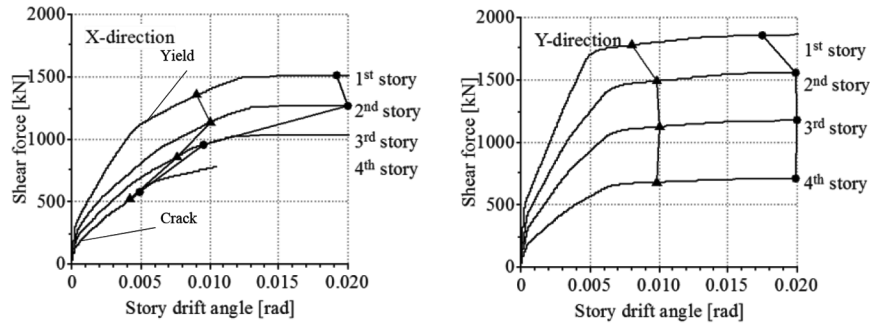
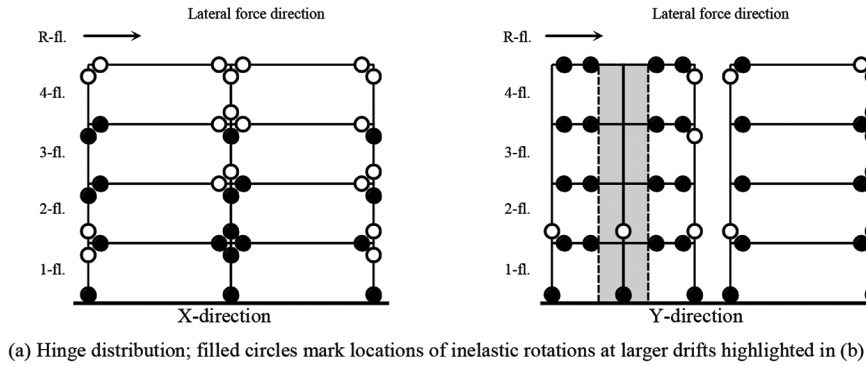


Fig. 3—Pushover analysis results. (Note: 1 kN = 0.225 kip.)

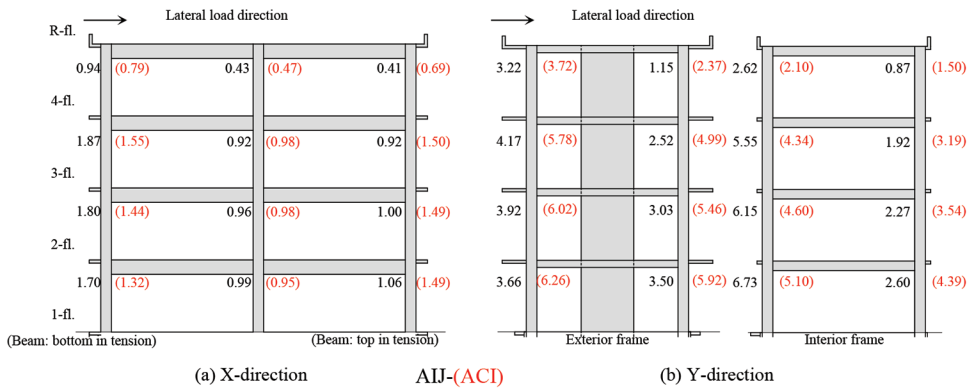


Fig. 4—Moment strength ratios of columns to beams.

goal was to determine how well the structure compares with U.S. seismic design practices. Rather than presume that the building was to be constructed at a particular site with corresponding site seismic hazard, the assessments of seismic design requirements are based on a seismic hazard represented by the linear response spectrum for the 100% JMA-Kobe ground motion to which the test structure was subjected.

Shear wall direction (y-direction)—The approximate natural period in the shear wall direction is 0.31 seconds based on Eq. 12.8-7 in ASCE 7-10. The spectral acceleration corresponding to this period is approximately 2.5g for the 100% JMA-Kobe ground motion imparted to the structure (Fig. 5, y-direction). Elastic analysis was performed using equivalent (static) lateral forces corresponding to the spectral acceleration divided by an *R* factor of 6, as specified in ASCE 7-10 for a building frame system with special rein-

forced concrete shear walls. Equivalent lateral forces were distributed over the height of the structure in accordance with provisions of ASCE 7-10. An effective moment of inertia equal to 50% of the gross moment of inertia was used over the full wall height: an intermediate value between the effective moments of inertia provided in ACI 318-11 for cracked and uncracked walls. Selected wall effective moments of inertia are also consistent with values recommended by ASCE 41-06 (ASCE/SEI Committee 41 2007a) for cracked walls. An effective moment of inertia equal to 30% of the gross moment of inertia was used for beams and columns as per ASCE 41-06 (ASCE/SEI Committee 41 2007b) – supplement 1) provisions for beams and columns with low axial loads. Beams were considered T-beams with an effective flange width evaluated in accordance with provisions of ACI 318-11. Joints were taken as rigid. Elastic analysis of the walls decoupled from frames at Axes A and C indicates

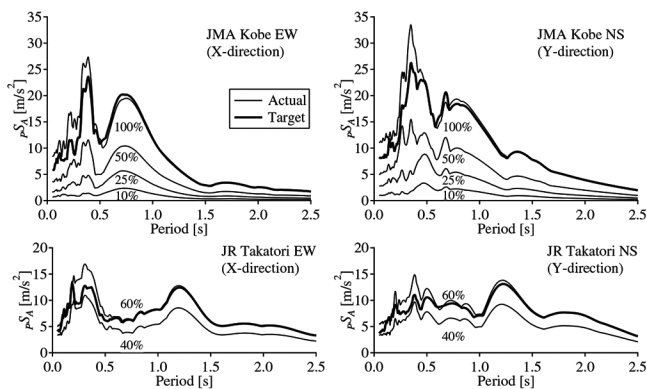


Fig. 5—Acceleration response spectra of input waves. (Note: Damping ratio = 0.05; $1 \text{ m/s}^2 = 39.37 \text{ in./s}^2$.)

that the walls would develop their design moment strength ($0.9 \times$ nominal moment strength) at approximately $0.37/R$ of the JMA-Kobe 100% motion. If wall-frame interaction is taken into account, however, the wall-frame system would develop its design moment strength at approximately $0.55/R$ of the 100% JMA-Kobe motion. Thus, the building in the wall direction has only 55% of the strength that would be required for the JMA-Kobe motion if that motion is considered as the design earthquake shaking level. In subsequent discussion, wall-frame interaction is taken into account. When applying the equivalent lateral-force distribution in accordance with ASCE 7-10, wall flexural yielding occurs at a lower load than that generating the wall's factored shear strength. Distributed vertical and horizontal steel satisfied all shear reinforcement requirements of ACI 318-11.

The wall-foundation interface was not intentionally roughened prior to casting the walls. Given the amount of longitudinal steel crossing the interface, the axial force on the walls, and a friction coefficient of 0.6, nominal shear-friction strength in accordance with ACI 318-11 of both wall bases was approximately 2140 kN (482 kip). That shear-friction strength exceeded estimated shear demands by approximately 55% based on the 100% JMA-Kobe ground motion. Nominal shear-friction strength was, however, only 20% higher than maximum base shear demand estimated from pushover analysis (approximately 1800 kN [405 kip]), which accounts to some extent for member over-strength.

ACI 318-11 allows the use of two methods to determine if boundary elements are required in walls. If the drift-based method is considered (ACI 318-11, Section 21.9.6.2), no boundary elements are required in the walls for the 100% JMA-Kobe motion, whether drift estimates are obtained considering wall-frame interaction or not. If the stress-based method is considered (ACI 318-11, Section 21.9.6.3), however, boundary elements are required in the walls up to a height of 7550 mm (297 in.) from the base of the wall if walls are considered decoupled from the frames, and a height of 5060 mm (199 in.) if wall-frame interaction is accounted. If one considers that boundary elements are not required in the walls, minimum boundary detailing in both walls satisfies ACI 318-11 provisions. If one considers that boundary elements are required, however, the provided spacing of hoops in the boundary elements of the wall at Axis C (100 mm [3.94 in.]) marginally exceeds the required spacing

(83 mm [3.26 in.]). In the wall at Axis A, hoops were spaced at 80 mm (3.15 in.) in the first story and this spacing satisfies all ACI 318 hoop spacing requirements for the boundary element. In the upper stories of the wall at Axis A, hoops in the boundary regions were spaced at 100 mm (3.93 in.) and therefore did not satisfy the ACI 318-required spacing of 83 mm (3.26 in.).

If wall-frame interaction was considered, beams spanning between shear walls and corner columns were found to have sufficient moment strength to resist moments from elastic analysis based on the 100% JMA-Kobe motion hazard level. Shear strengths of the beams were sufficient to develop beam probable moment strengths.

Because demands on corner columns in the shear wall direction were significantly lower than demands on the same columns in the frame direction, capacity and detailing of corner columns will be described in the section discussing the frame direction (x-direction).

Frame direction (x-direction)—The approximate natural period in the moment frame direction is 0.44 seconds based on ASCE 7-10 Eq. 12.8-7. The spectral acceleration corresponding to this period is approximately 1.45g for the 100% JMA-Kobe ground motion imparted to the structure (Fig. 5, x-direction). Elastic analysis was performed using equivalent (static) lateral forces corresponding to the spectral acceleration divided by an R factor of 8, as specified in ASCE 7-10 for special reinforced concrete moment frames. Equivalent lateral forces were distributed over the height of the structure in accordance with ASCE 7-10. Elastic analysis of the frames indicates that the first-story corner columns reach design flexural strength at a shaking level corresponding to approximately $1.4/R$ of the JMA-Kobe 100% motion. All frame member strengths therefore exceeded the required design strength corresponding to a 100% JMA-Kobe hazard level.

Factored shear strengths of all beams were not sufficient to develop probable moment strengths due to the requirement that concrete shear contribution be taken as zero (ACI 318-11, Section 21.5.4.2). Maximum beam shear stresses corresponding to the development of probable moment strengths ranged from 2.0 to 2.7 times the square root of the concrete compressive strength in psi (0.17 to 0.22 MPa). The spacing of beam transverse reinforcement was 200 mm (7.87 in.) in the critical plastic hinge regions, which exceeds the maximum allowable spacing of 120 mm (4.72 in.) as required by ACI 318-11.

Factored shear strengths of the third- and fourth-story columns were not sufficient to develop probable moment strengths. Column shear stresses corresponding to the development of column probable moment strengths ranged from 1.4 to 3.8 times the square root of the concrete compressive strength in psi (0.114 to 0.315 MPa). Column-end transverse reinforcement met spacing and layout requirements of ACI 318-11 in the first two stories but not the top two stories. No columns met the requirement for minimum volumetric reinforcement ratio in the critical end regions; columns had 20 to 50% of the hoop volumes required by ACI 318-11 in the critical end regions. Transverse reinforcement ratios varied substantially between columns in different stories due to differences in numbers of crossties.

Table 4—Key response values at roof

Test No.	Input wave	Maximum roof acceleration		Maximum roof drift*		Residual roof drift	
		x-direction, m/s ²	y-direction, m/s ²	x-direction, mm	y-direction, mm	x-direction, mm	y-direction, mm
1	JMA-Kobe 25%	3.12	6.37	16.9	24.2	0.5	0.4
2	JMA-Kobe 50%	7.03	11.01	122.4	106.9	1.1	5.4
3	JMA-Kobe 100%	9.65	14.01	242.7	323.9	6.2	22.5
4	JR-Takatori 40%	6.46	8.13	240.4	240.8	1.3	7.9
5	JR-Takatori 60%	8.09	9.99	278.1	414.0	8.0	11.6

*Maximum roof drifts do not include residual drifts accrued from previous tests.

Notes: 1 m²/s = 39.37 in./s²; 1 mm = 0.039 in.

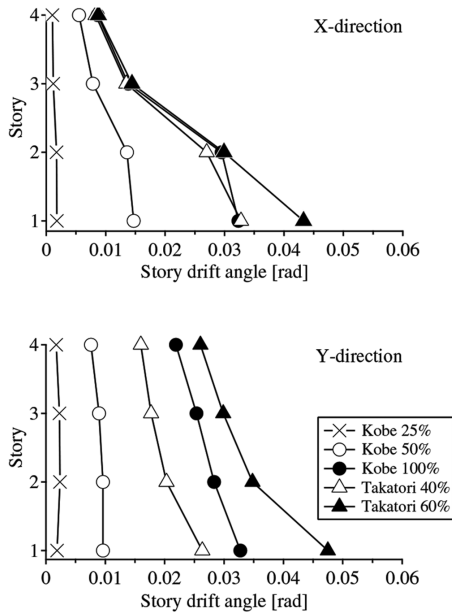


Fig. 6—Maximum inter-story drift distribution.

Joint shear demands for both interior and exterior joints were calculated considering force equilibrium on a horizontal plane at the midheight of the joints, in accordance with ACI 318-11. Joint shear demands calculated including the contribution of slab flexural tension reinforcement within the ACI 318 effective flange width were found to be approximately 20 to 40% higher than demands computed ignoring the slab contribution. Note that ACI 318 does not require consideration of the slab reinforcement in calculations of joint shear demand. Regardless of whether slab contribution was taken into account, all joint design shear strengths, based on ACI 318-11, exceeded joint shear demands. Because joints were only confined by hoops without crossties, the maximum center-to-center horizontal spacing between hoop or crosstie legs was larger than the ACI 318-11 limit of 350 mm (14 in.). The provided hoop spacing in the joints of 140 mm (5.5 in.) was larger than the maximum spacing allowed by ACI 318-11 of approximately 25 mm (1 in.) for the provided arrangement of hoops without crossties (limited by minimum volumetric reinforcement ratio requirements). Other joint detailing satisfied ACI 318-11 requirements, including those for longitudinal bar anchorage.

Figure 4 shows column-beam nominal moment strength ratios. Below the roof, all strength ratios for exterior columns

satisfied the 6/5 minimum requirement of ACI 318-11. That requirement was not satisfied at interior joints.

E-DEFENSE SHAKE-TABLE FACILITY AND TEST CONDITIONS

The E-Defense shake-table facility has been operated by the National Research Institute for Earth Science and Disaster Prevention of Japan since 2005. The table is 20 x 15 m (65 ft 7 in. x 49 ft 3 in.) in plan dimension and can produce a velocity of 2.0 m/s (78.7 in./s) and a displacement of 1.0 m (39.4 in.) in two horizontal directions simultaneously. It can accommodate a specimen weighing up to 1200 tonnes (1323 tons). In this series of tests, the considered reinforced concrete building was tested side-by-side with a prestressed concrete building having almost the same configuration and overall dimensions (Fig. 2). More detail about the test structure, including detailed drawings, can be found in Nagae et al. (2011b).

LOADING PROGRAM

Ground motions designated as JMA-Kobe and JR-Takatori, recorded in the 1995 Hyogoken-Nanbu earthquake, were adopted as the input base motions. The North-South-direction wave, East-West-direction wave, and vertical-direction wave were input to the y-direction, x-direction, and vertical direction of the specimen, respectively. The intensity of input motions was gradually increased to observe damage progression. The adopted amplitude scaling factors for JMA-Kobe were 10, 25, 50, and 100%. Following the JMA-Kobe motions, the JR-Takatori motion scaled to 40 and 60% was applied to impart large cyclic deformations. Figure 5 presents the acceleration response spectra for the input motions. JMA-Kobe 100% has a strong intensity in the short-period range corresponding to the natural period of the specimen, as can be seen in Fig. 5. The JR-Takatori 60% has a strong intensity in the longer-period ranges corresponding to estimated damaged specimen periods.

TEST RESULTS

Maximum recorded story drift and global behavior

White-noise inputs were applied prior to each main test. From these, the initial natural periods of the test building were found to be 0.43 seconds in the frame direction and 0.31 seconds in the wall direction, which compare favorably with periods estimated using ASCE 7-10 Eq. 12.8-7 (0.44 seconds in the frame direction and 0.31 seconds in the wall

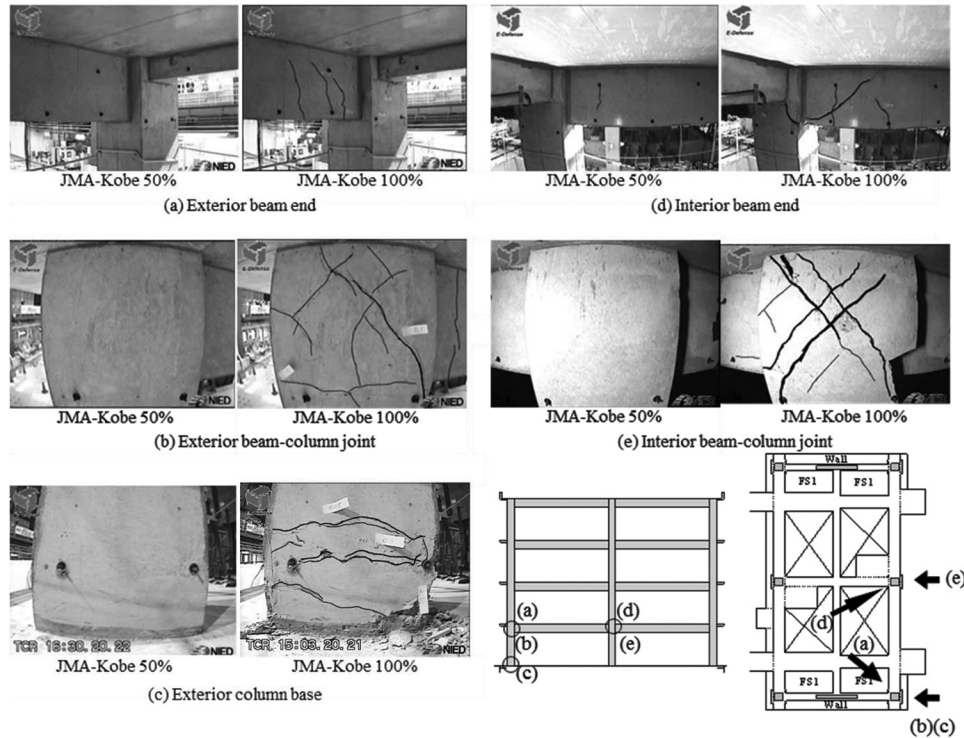


Fig. 7—Damage state of moment frame with cracks highlighted.

direction). Figure 6 shows the distribution of maximum story drift over the height of the specimen for the shaking tests. In the frame direction, the story drift is larger in the first and second stories than in the third and fourth stories. In the wall direction, the story drifts are relatively uniform, although the drifts become larger in the first story than drifts of other stories in the JMA-Kobe 100% test and JR-Takatori tests. The structure remained stable through all the severe dynamic tests and thus satisfied the minimum collapse-prevention performance objective. Table 4 lists the maximum recorded roof level accelerations, drifts, and residual drifts for all earthquake simulation tests. Residual drifts were relatively low, with a maximum recorded value of 22.5 mm (0.88 in.) in the wall direction at the end of the JMA-Kobe 100% motion.

Damage states of members

Figures 7 through 9 show images of damage in the lower parts of the specimen. After the JMA-Kobe 50% test, the interior beam-column joints of the second floor and the column and wall bases of the first story showed minor cracking. In the interior beam-column joints, the maximum measured inclined crack width of 0.5 mm (0.02 in.) after the JMA-Kobe 50% test increased to 2.5 mm (0.1 in.) after the JMA-Kobe 100% test. Eventually, inclined cracks in the interior beam-column joints at the second floor reached 5.3 mm (0.21 in.) after the JR-Takatori 60% test. Maximum inclined crack widths at beam ends and exterior beam-column joints were limited to about 1.5 mm (0.06 in.), even after the JR-Takatori 60% test. Compressive failure of concrete apparently due to large flexural deformations was observed in column and wall bases. The cover concrete of column bases partially spalled to a height of 250 mm (9.8 in.) in the JMA-Kobe 100% test,

and completely spalled to a height of 200 to 400 mm (7.9 to 15.8 in.) in the JR-Takatori 60% test. The core concrete of column bases remained adequately confined by transverse reinforcement even after the JR-Takatori 60% test.

The corner portion of both wall bases suffered compressive failure to a height of 300 mm (11.8 in.) and length of 600 mm (23.6 in.) in the JMA-Kobe 100% test. The longitudinal reinforcement in that region had lateral offset due to inelastic buckling. Wall sliding at both wall bases was observed in the JMA-Kobe 100% and subsequent tests. Significant sliding was primarily observed following crushing of the wall boundary zones (Wallace 2012), which may have weakened the wall-foundation interface shear friction resistance. The sliding mechanism affected the maximum drift and deformation demands in the test structure and may have accentuated the damage observed in the wall boundary regions. Sliding of the walls at their base reached approximately 100 mm (3.93 in.) during the JMA-Kobe 100% test and accounted for up to 10% of the roof drifts during that motion.

Local deformations

The shear deformations of the second-floor interior joints are highlighted first because these joints sustained severe damage and degradation. Shear deformations of the second-floor interior beam-column joints were measured in the frame direction, as shown in Fig. 8(a). Figure 8(b) shows the history of the shear deformation angles as well as the average story drift angles of the upper and lower stories during the JMA-Kobe 100% test. Peaks a to e in the response history (Fig. 8(b)) are identified for later reference. Assuming that the shear deformation angle of the beam-column joint contributes to the average story drift angle, as shown in Fig. 8(c), the deformation ratio is defined as the

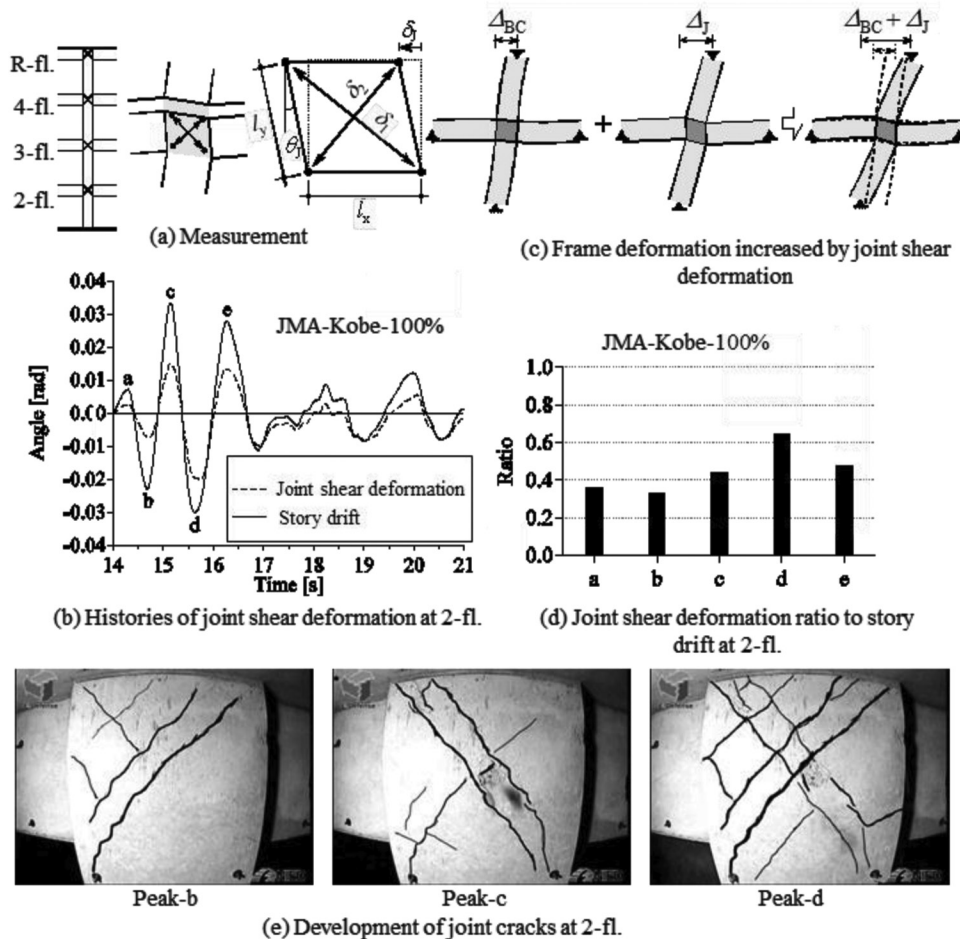


Fig. 8—Deformation of interior beam-column joint in JMA-Kobe 100%.

ratio of the shear deformation angle to the average story drift angle. Figure 8(d) shows the deformation ratio from Peaks a to e. The deformation ratio was 0.35 at Peak a (when the average story drift ratio reached 0.009) and reached more than 0.6 at Peak d. Figure 8(e) shows the development of inclined cracks in the joint at Peaks b, c, and d.

The rotation and lateral slip deformations of the wall base were measured in the y-direction using instrumentation shown schematically in Fig. 9(a). The histories of the base rotation angle, lateral slip, and first-story drift and drift angle during the JMA-Kobe 100% test are shown in Fig. 9(b) and (f). Peaks of story drift are denoted a to g for cross reference with other figures. Figure 9(c) shows an overall photograph of the wall at Peak c. A local compressive failure is seen at the base corner of the A-side, and several tension cracks are seen at the lower part of the B-side. Figure 9(d) shows the deformation ratio at the peak story drifts in the JMA-Kobe 100% test. The deformation ratio is defined as the ratio of drift due to base rotation and lateral sliding to story drift. At Peak c, the story drift was mostly derived from the rotation and lateral sliding of the wall base. Because the maximum lateral sliding displacement becomes approximately constant after the maximum deformation of Peak c, the deformation ratio of lateral sliding increased at Peaks e and g. Figure 9(e) shows the damage of a wall base after the test. From video observations, lateral sliding became significant at Peak c and

the local buckling of bars occurred at the base of B-side in the cycle when the story drift approached Peak d.

Global hysteretic behavior and strength

The global drift angle is defined as the relative horizontal displacement of the fourth floor level (Fig. 1) divided by its height above the base. The base shear force was calculated based on the horizontal inertia forces given by the estimated weight of each floor and the corresponding floor accelerations. In shear force calculations, the weights of vertical elements were lumped with floor weights as presented in Table 1.

Figure 10 shows the relationship between the base shear force and global drift angle. In the relationships, the hysteretic loops show inelastic behavior, while the stiffness is observed to decrease with an increase in the drift angle, as evinced by the decrease in reloading stiffness with increasing drift angles. The history of story shear force (Fig. 10) indicates that the elongation of the first-mode period is more significant in the frame direction than in the wall direction in the JMA-Kobe 50% test, while the period in the wall direction elongated noticeably in the JMA-Kobe 100% test due to the damage incurred by the shear walls. The apparent lowest periods of the structure estimated by the white-noise input were 0.99 seconds in the frame direction and 0.88 seconds in the wall direction after the JMA-Kobe 100% test. It is useful to note that measured base shear forces reached a maximum of approximately 85% of the building weight

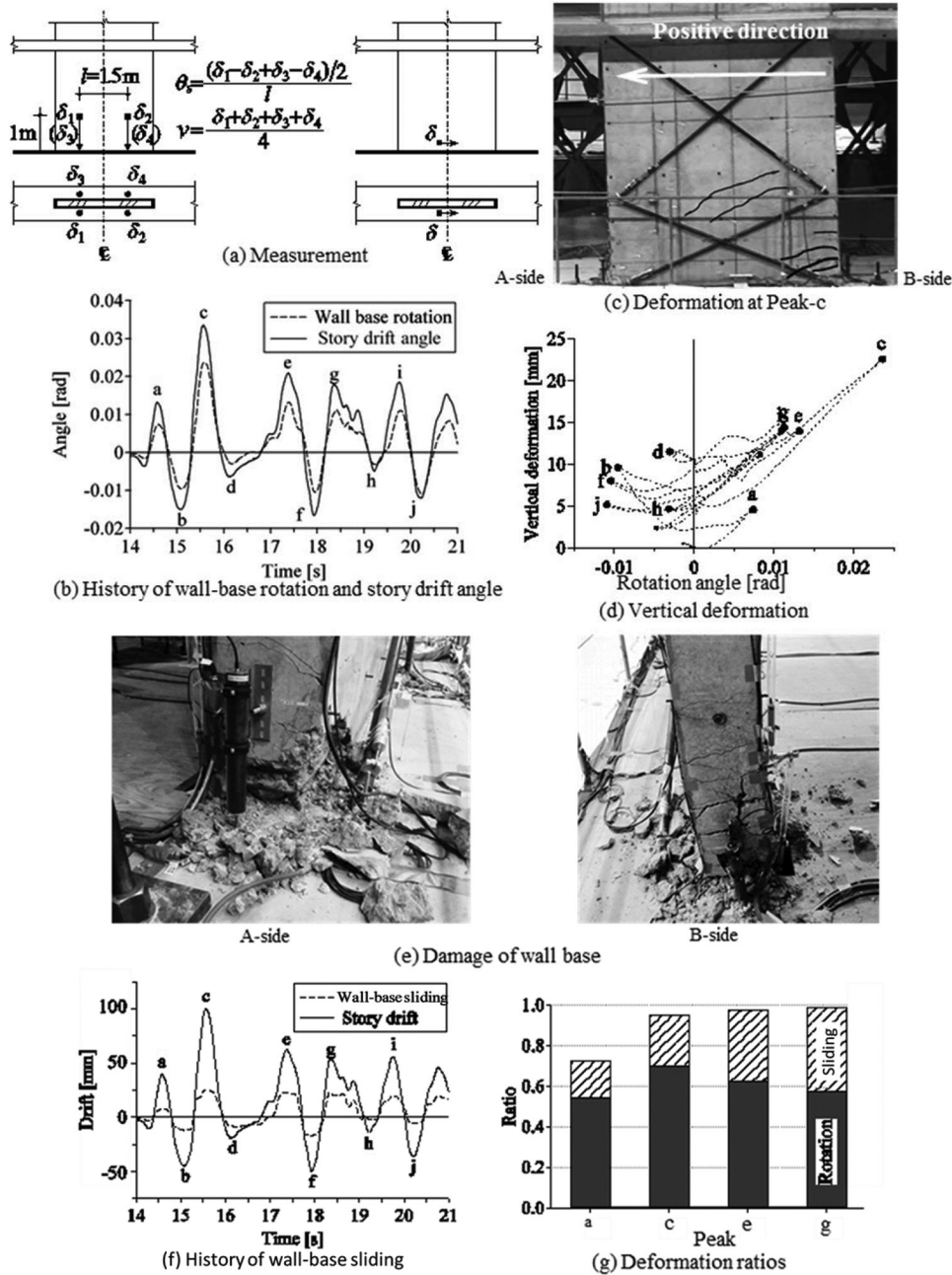


Fig. 9—Deformation of wall base in JMA-Kobe 100%. (Note: 1 mm = 0.039 in.)

in the wall direction and 55% in the frame direction. Thus, actual strength was well in excess of the design lateral force level of $0.2W$ in each direction.

Figure 11 shows the distribution of the story shear coefficient over the height of the structure. The story shear coefficient is defined as the story shear force divided by the weight of the floors above that story, normalized by the value of the coefficient at the first story. The figure presents values of the coefficient evaluated using the maximum story shear forces recorded during a given motion (“Max” in the figure), and values of the coefficient evaluated using story shear forces occurring at the same time instant when the base shear reaches its maximum (“Base Peak” in the figure). Also presented in the figure are the design shear coefficients prescribed in Japanese design practice (given by the factor A_i in the 2007 MLIT standard). Equivalent story shear coef-

ficients estimated using the ASCE 7-10 equivalent lateral-force procedures are also shown in the figure. It is useful to note that the distribution of the story shear coefficients corresponds to a similar distribution of applied floor inertia forces; for example, an inverted triangular distribution of story shear force coefficients implies an inverted triangular distribution of floor inertia forces. Figure 11 indicates that floor inertia forces at peak base shear had a relatively uniform distribution over the height of the building, as opposed to an inverted triangular distribution often assumed in design, especially in the JMA-Kobe 100% and the JR-Takatori 60% tests. Such uniform vertical seismic force distributions have been observed in previous shake-table tests (for example, Kabeyasawa et al. 1984). Higher mode contributions and localization of damage may have influenced the observed vertical distribution of lateral forces. Such observation

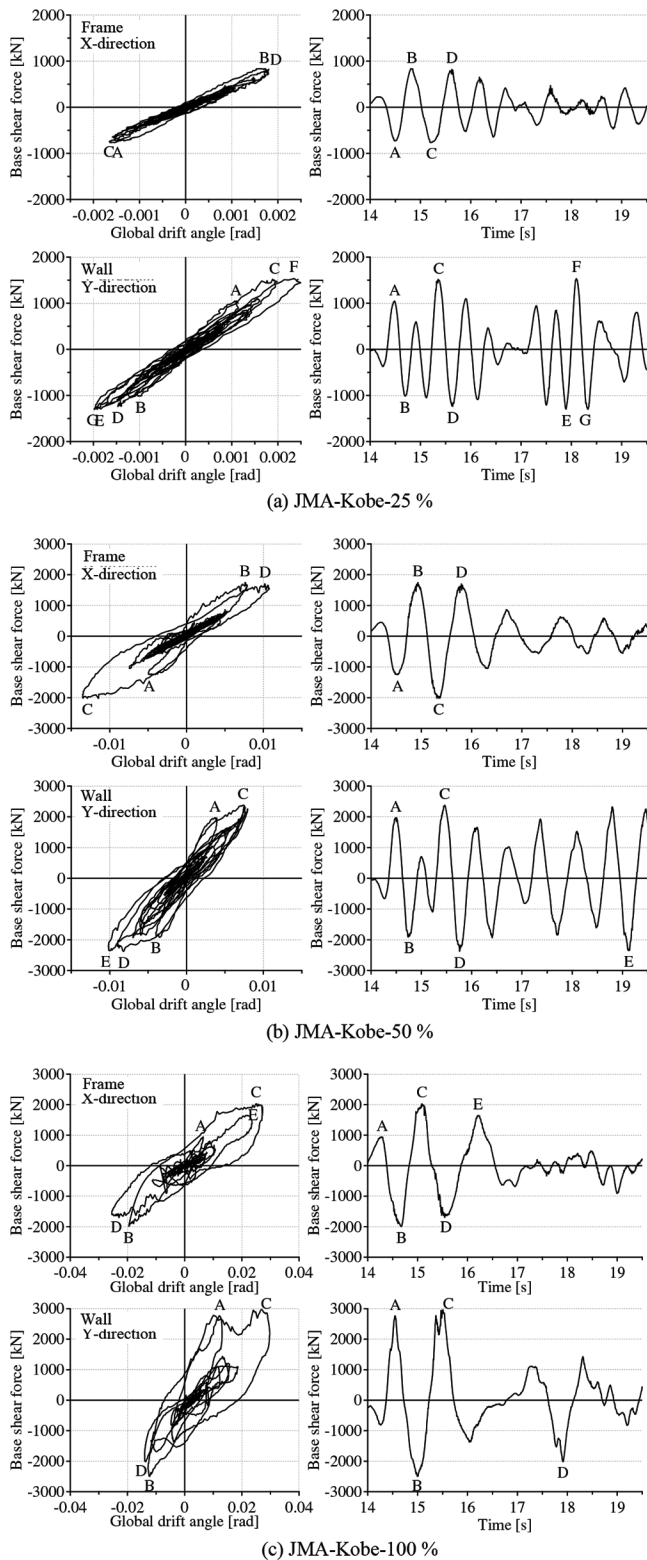


Fig. 10—Hysteretic behavior and history of base shear force. (Note: 1 kN = 0.225 kip.)

can partly explain the higher than estimated base shear forces seen in Fig. 10. This is particularly the case in the wall direction where observed base shear forces during the JMA-Kobe 100% motions were more than 50% larger than those estimated from pushover analysis; which was based on an approximate inverted triangular lateral load distribution (Fig. 3).

Overtuning moment at the base of the first story is mostly produced by the first-mode response of a structure and is relatively insensitive to the distribution of the lateral forces (Kabeyasawa et al. 1984). Roof drift is also relatively insensitive to higher modes. Thus, the relation between roof drift angle and base moment is a convenient measure for comparing calculated and laboratory test strengths. Figure 12 shows the measured relationships between roof drift angle and overturning moment. Calculated overturning moments, obtained by pushover analyses at maximum story drift ratio of 0.02 (Fig. 4), are also shown in Fig. 12. In the y-direction, the measured maximum overturning moment is 1.3 times the calculated value, while in the x-direction, the measured maximum overturning moment is 1.5 times the calculated value. Several factors may have contributed to the measured overstrength, including underestimation of the slab contribution to member strengths, other three-dimensional effects, and strain-rate effects.

IMPLICATIONS OF TEST RESULTS TO ACI 318-11

Although columns had 20 to 50% of the hoop volumes required by ACI 318-11 in the critical end regions, they performed adequately, maintaining core integrity through the full series of severe dynamic tests. It is noted, however, that column axial forces were relatively low, varying from an estimated tensile force on corner columns due to uplift, to a maximum compressive axial force of approximately $0.1A_gf'_c$ at the first story (where A_g is the column gross-section area and f'_c is the measured concrete compressive strength). This observation suggests that the volume of transverse reinforcement required by ACI 318-11 may be reduced in the axial force ranges of the tested columns. Several design codes (including the Japanese MLIT Standard 2007, CSA A.23.3-04 (2004), and NZS 3101 2006 (2006a,b)) account for the effects of axial force on confinement requirements of concrete columns. While these codes treat the effects of axial forces in different ways, they generally require less confinement reinforcement for lower axial forces.

Similarly, the volume ratios of hoops in the critical regions of the beams were 60% of the ratios required. Beams performed adequately and suffered relatively minor damage while maintaining core integrity throughout the dynamic tests. It is important to note that the beams were under relatively low shear stresses. Such observations indicate that beams under low shear stresses and conforming to the principles of ACI 318-11 but with somewhat lighter transverse reinforcement can meet life-safety performance objectives.

Both shear walls sustained notable damage, including cover spalling and bar buckling, during the first high-intensity ground motion (JMA-Kobe 100%). It is noteworthy that confined boundary elements were not even required by the ACI 318 provisions (using the displacement-based approach). One of the reasons for the inconsistency here is that the measured lateral displacements were approximately twice the design values. Considering the measured displacements, ACI 318 provisions would have required confined boundary elements.

Although confinement was not required by the ACI 318 provisions, the wall boundaries nonetheless contained

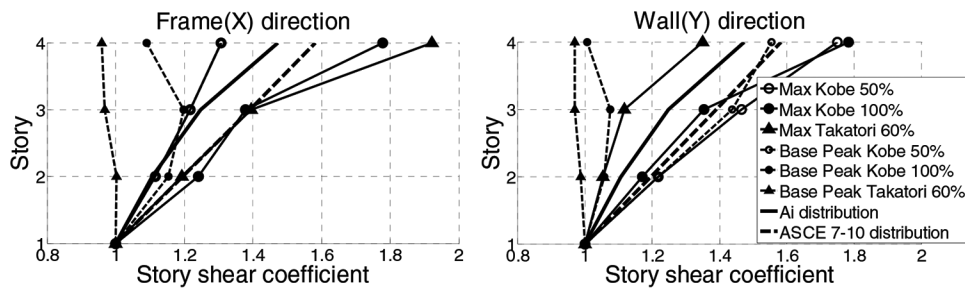


Fig. 11—Distribution of floor lateral force coefficient.

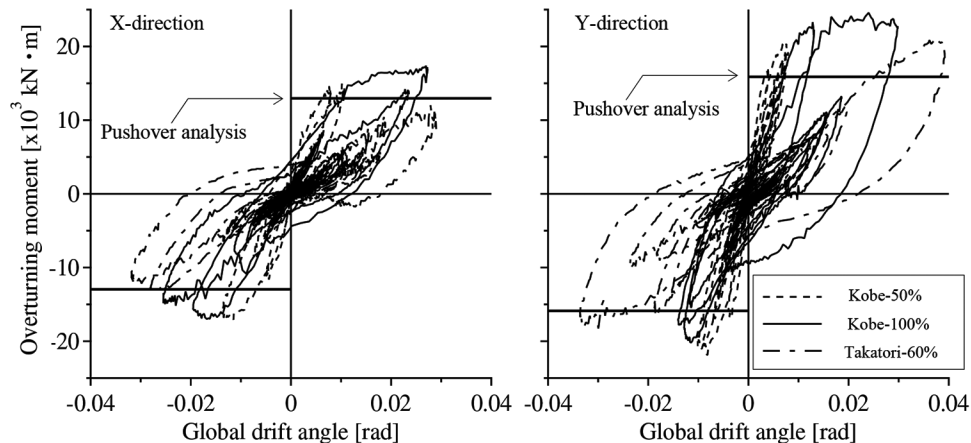


Fig. 12—Hysteretic behavior based on overturning moment. (Note: 1 kN-m = 0.737 k-ft.)

confinement reinforcement satisfying the ACI 318 special boundary element requirements at Axis A and nearly satisfying them at Axis C. The observed concrete spalling and longitudinal reinforcement buckling exceeded expectations of some of the authors, and may suggest a need for improved detailing requirements.

The nominal shear-friction strength at the wall-foundation interface, calculated in accordance with ACI 318-11, was 2140 kN (482 kip) for both walls combined. Shear demands on the first story were estimated to be 1400 kN (315 kip) based on the JMA-Kobe 100% ground motion being the design motion, 1800 kN (405 kip) based on pushover analysis, and 3000 kN (675 kip) based on recorded data. Measured base shear demands were 40% larger than the calculated shear-friction capacity of the wall-foundation interface. Test data therefore indicate that improvements on methods for estimating peak shear demands on wall systems should be sought. Notably, the effects of higher modes and localized damage on the vertical distribution of lateral loads should be considered when estimating peak story-shear demands.

The interior beam-column joints sustained significant damage during the earthquake simulation tests. Implications for ACI 318 are not readily extracted, however, because the beam-column joint designs did not satisfy the ACI 318 requirements. Deficiencies included deficient ratios of column-beam flexural strength ratios and deficient volumetric ratio of joint transverse reinforcement.

SUMMARY AND CONCLUSIONS

A full-scale, four-story, reinforced concrete building structure was tested on the E-Defense shake table. The structure was designed in accordance with the present Japanese seismic

design code. Minor adjustments to the design were made to bring the final structure closer to U.S. practice and thereby benefit a broader audience. The structure was subjected to a series of multi-directional seismic base motions including three high-intensity motions. The following key observations were made:

1. The structure remained stable throughout the tests, even though lateral drift ratios exceeded 0.04. Thus, the structure satisfied a collapse-prevention performance objective. The structure did, however, sustain severe damage in the walls and beam-column joints.

2. At times of maximum base shear, the distribution of lateral inertia forces was approximately uniform over height, unlike the inverted triangular distribution used to design the structure. The nearly uniform lateral force distribution, along with other factors, resulted in a significant increase in the maximum base shear during the tests. Test data therefore indicate that improvements on methods for estimating peak shear demands on wall systems should be sought.

3. Both walls suffered significant damage in their boundary regions, including wall boundary crushing, longitudinal reinforcement buckling, and lateral instability. Walls had tightly spaced hoop reinforcement at the boundaries that satisfied all ACI confinement requirements at Axis A and nearly satisfied them at Axis C. ACI 318-11 provisions for the transverse reinforcement of special structural walls may need to be adjusted if more limited damage is desired, particularly for thin walls with relatively large cover.

4. Significant sliding at the wall-foundation construction joint was observed at the base of both walls. The sliding mechanism affected the maximum drift and deformation demands in the test structure and may have accentuated

the damage observed in the wall boundary regions. Three factors may have contributed to the observed sliding. First, although the construction joint between the walls and the foundation were cleaned, they were not intentionally roughened as required by ACI 318-11. Second, although design shear demands were less than the sliding shear strength calculated in accordance with ACI 318-11, the actual test shears were much higher than the design values. Third, damage to the wall-boundary regions may have reduced the shear-friction strength at the wall-foundation joints. These observations suggest two issues that may not be adequately treated in current codes. First, that higher-mode contributions and effects of localized damage should be accounted for when estimating shear force demands on shear walls, and second, that integrity and stability of the wall boundary zone is an important component of wall sliding shear resistance.

5. Columns performed adequately and maintained core integrity throughout the series of severe tests even though they did not satisfy the confinement volumetric reinforcement ratio requirements of ACI 318-11. Column axial force ratios were relatively low and did not exceed 10% of the column gross-section axial capacity. Test results therefore indicate that it might be possible to reduce the ACI 318-11 minimum volumes of confining reinforcement for columns with low axial force ratios.

6. Beams also performed adequately and maintained core integrity even though they did not satisfy the confinement volumetric reinforcement ratio requirements of ACI 318-11. Beam shear stresses were, however, relatively low and did not exceed 2.7 times the square root of concrete compressive strength in psi units (0.22 in MPa units).

7. Joints performed poorly, exhibiting wide inclined cracks and deformations that accounted for up to 60% of floor drifts at the end of the test series. Interior joints performed worse than exterior joints. It is noted that the joint designs satisfied Japanese code requirements but did not satisfy ACI 318-11 code requirements.

AUTHOR BIOS

T. Nagae is a Senior Researcher at the National Research Institute for Earth Science and Disaster Prevention, Tsukuba, Japan.

W. M. Ghannoum is an Assistant Professor at the University of Texas at Austin, Austin, TX.

J. Kwon is a PhD Candidate at the University of Texas at Austin.

K. Tahara is a Researcher at the National Research Institute for Earth Science and Disaster Prevention.

K. Fukuyama is a Visiting Researcher at the National Research Institute for Earth Science and Disaster Prevention.

T. Matsumori is a Senior Researcher at the National Research Institute for Earth Science and Disaster Prevention.

H. Shiohara is a Professor at the University of Tokyo, Tokyo, Japan.

T. Kabeyasawa is a Professor at the University of Tokyo.

S. Kono is a Professor at the Tokyo Institute of Technology, Tokyo, Japan.

M. Nishiyama is a Professor at Kyoto University, Kyoto, Japan.

R. Sause is a Professor at Lehigh University, Bethlehem, PA.

J. W. Wallace is a Professor at the University of California, Los Angeles, Los Angeles, CA.

J. P. Moehle is the T.Y. and Margaret Lin Professor at the University of California, Berkeley, Berkeley, CA.

ACKNOWLEDGMENTS

The authors acknowledge the generous support of the Ministry of Education, Culture, Sports, Science & Technology (MEXT) and of the National Research Institute for Earth Science and Disaster Prevention of Japan for carrying out the tests presented in this paper. Participation by the U.S. co-authors was supported by the Pacific Earthquake Engineering Center and by the Network for Earthquake Engineering Simulation of the National Science Foundation under award CMMI-1000268. Additional instrumentation of the test structure using NEES@UCLA sensors was provided under Award CMMI-1110860, while analysis of the data was partly funded by the National Science Foundation under Award No. 1201168. Any opinions, findings, and conclusions or recommendations expressed in this material are those of the authors and do not necessarily reflect the views of the sponsors.

REFERENCES

ACI Committee 318, 2011, "Building Code Requirements for Structural Concrete (318-11) and Commentary," American Concrete Institute, Farmington Hills, MI, 503 pp.

AIJ, 1999, "Design Guidelines for Earthquake Resistant Reinforced Concrete Buildings Based on the Inelastic Displacement Concept," Architectural Institute of Japan, Tokyo, Japan, 440 pp. (in Japanese)

AIJ, 2010, "Standard for Structural Calculation of Reinforced Concrete Structures," Architectural Institute of Japan, Tokyo, Japan, 526 pp. (in Japanese)

ASCE/SEI Committee 41, 2007a, "Seismic Rehabilitation of Existing Structures (ASCE/SEI 41-06)," American Society of Civil Engineers, Reston, VA, 428 pp.

ASCE/SEI Committee 41, 2007b, "Supplement to Seismic Rehabilitation of Existing Buildings (ASCE/SEI 41-06)," American Society of Civil Engineers, Reston, VA, 428 pp.

ASCE/SEI Committee 7, 2010, "Minimum Design Loads for Buildings and Other Structures (ASCE/SEI 7-10)," American Society of Civil Engineers, Reston, VA, 636 pp.

CSA A23.3-04, 2004, "Design of Concrete Structures," Canadian Standards Association, Mississauga, ON, Canada, 258 pp.

Kabeyasawa, T.; Shiohara, H.; and Otani, S., 1984, "U.S.-Japan Cooperative Research on R/C Full-Scale Building Test, Part 5: Discussion of Dynamic Response System," *Proceedings of the 8th World Conference on Earthquake Engineering*, San Francisco, CA, pp. 627-634.

MLIT, 2007, "Technological Standard Related to Structures of Buildings," Ministry of Land, Infrastructure, Transport, and Tourism, Tokyo, Japan.

Nagae, T.; Tahara, K.; Fukuyama, K.; Matsumori, T.; Shiohara, H.; Kabeyasawa, T.; Kono, S.; Nishiyama, M.; and Nishiyama, I., 2011a, "Large-Scale Shaking Table Tests on A Four-Story RC Building," *Journal of Structural and Construction Engineering*, V. 76, No. 669, pp. 1961-1970. doi: (Transactions of AIJ)10.3130/aijs.76.1961

Nagae, T.; Tahara, K.; Taiso, M.; Shiohara, H.; Kabeyasawa, T.; Kono, S.; Nishiyama, M.; Wallace, J. W.; Ghannoum, W. M.; Moehle, J. P.; Sause, R.; Keller, W.; and Tuna, Z., 2011b, "Design and Instrumentation of the 2010 E-Defense Four-Story Reinforced Concrete and Post-Tensioned Concrete Buildings," *PEER Report 2011/104*, Pacific Earthquake Engineering Research Center (PEER), Berkeley, CA, 261 pp.

NEEShub project 2011-1005, "U.S. Instrumentation and Data Processing for the Four-Story Reinforced Concrete and Post-Tensioned E-Defense Building Tests," The George E. Brown, Jr. Network for Earthquake Engineering Simulation, <https://nees.org/warehouse/report/project/1005>. (last accessed Feb. 2014)

NZS3101, Part 1:2006, 2006a, "Concrete Structures Standard: Part 1—The Design of Concrete Structures," Standards Association of New Zealand, Wellington, New Zealand, 309 pp.

NZS3101, Part 2:2006, 2006b, "Concrete Structures Standard—Commentary," Standards Association of New Zealand, Wellington, New Zealand, 397 pp.

Tuna, Z., 2012, "Seismic Performance, Modeling, and Failure Assessment of Reinforced Concrete Shear Wall Buildings," PhD dissertation, University of California, Los Angeles, Los Angeles, CA, 298 pp.

Wallace, J. W., 2012, "Behavior, Design, and Modeling of Structural Walls and Coupling Beams—Lessons from Recent Laboratory Tests and Earthquakes," *International Journal of Concrete Structures and Materials*, V. 6, No. 1, pp. 3-18. doi: 10.1007/s40069-012-0001-4